

Soluble forms of VEGF receptor-1 and -2 promote vascular maturation *via* mural cell recruitment

Sophie Lorquet,^{*,†,1} Sarah Berndt,^{*,1} Silvia Blacher,^{*} Emily Gengoux,^{*} Olivier Peulen,^{*} Erik Maquoi,^{*} Agnès Noël,^{*} Jean-Michel Foidart,^{*,†,2} Carine Munaut,^{*} and Christel Péqueux^{*}

^{*}Laboratory of Tumor and Developmental Biology, GIGA-Cancer, University of Liège, Institute of Pathology, Liège, Belgium; and [†]Department of Gynecology and Obstetrics, University of Liège, CHR-Citadelle, Liège, Belgium

ABSTRACT Two soluble forms of vascular endothelial growth factor (VEGF) receptors, sVEGFR-1 and sVEGFR-2, are physiologically released and overproduced in some pathologies. They are known to act as anti-VEGF agents. Here we report that these soluble receptors contribute to vessel maturation by mediating a dialogue between endothelial cells (ECs) and mural cells that leads to blood vessel stabilization. Through a multidisciplinary approach, we provide evidence that these soluble VEGF receptors promote mural cell migration through a paracrine mechanism involving interplay in ECs between VEGF/VEGFR-2 and sphingosine-1-phosphate type-1 (S1P)/S1P1 pathways that leads to endothelial nitric oxide synthase (eNOS) activation. This new paradigm is supported by the finding that sVEGFR-1 and -2 perform the following actions: 1) induce an eNOS-dependent outgrowth of a mural cell network in an *ex vivo* model of angiogenesis, 2) increase the mural cell coverage of neovessels *in vitro* and *in vivo*, 3) promote mural cell migration toward ECs, and 4) stimulate endothelial S1P1 overproduction and eNOS activation that promote the migration and the recruitment of neighboring mural cells. These findings provide new insights into mechanisms regulating physiological and pathological angiogenesis and vessel stabilization.—Lorquet, S., Berndt, S., Blacher, S., Gengoux, E., Peulen, O., Maquoi, E., Noël, A., Foidart, J.-M., Munaut, C., Péqueux, C. Soluble forms of VEGF receptor-1 and -2 promote vascular maturation *via* mural cell recruitment. *FASEB J.* 24, 000–000 (2010). www.fasebj.org

Key Words: mural cell migration • vessel normalization • eNOS • NO • S1P1

IN HEALTHY TISSUES, ANGIOGENESIS generates perfused blood vessels and improves oxygenation (1). By contrast, tumor vasculature is abundant but disorganized, immature, and poorly efficient. Tumor vessels are tortuous and leaky and exhibit poor mural cell coverage (2). Tumor angiogenesis is therefore often “poorly productive” because nonfunctional vessel abnormality impairs oxygen supply (2). Tumor hypoxia, together

with hypoperfusion and increased interstitial pressure, impedes the delivery and the efficacy of anticancer drugs. Hypoxia also promotes invasion, metastasis, and malignancy (3). Vessel normalization has therefore gained interest as a therapeutic option to improve drug delivery and anticancer treatment (4). In addition to stabilizing vessels, the coverage of endothelial cells (ECs) by mural cells also reduces tumor cell intravasation (5–7). Clinical observations indicate that, besides triggering vessel pruning, antiangiogenic treatments targeting vascular endothelial growth factor (VEGF) signaling induce tumor vessel normalization, particularly by increasing vessel coverage by pericytes (PCs) (2, 4, 8–10). However, their mechanisms of action remain undefined.

The recruitment of mural cells, including PCs/smooth muscle cells (SMCs), involves various factors and their downstream molecular pathways, among which the main ones are platelet-derived growth factor (PDGF)-BB, basic fibroblast growth factor (bFGF), sphingosine-1-phosphate (S1P), angiopoietin-1 (Ang1), transforming growth factor (TGF)- β , and nitric oxide (NO) (11–15). In particular, growing evidence identifies S1P and its G-protein-coupled receptors as modulators of the cardiovascular system physiology (15). Gene deletion experiments demonstrate a key role of S1P type-1 receptor (S1P1) for the coverage of vessels by mural cells (16, 17). Recently, Mazzone *et al.* (6) reported that tumor vessels in animals with reduced expression of the oxygen sensor prolyl hydroxylase domain protein 2 (PHD2) are less leaky, have a better PC coverage and have a more consistent basement membrane, all hallmarks of mature, quiescent vessels. Decreasing the oxygen-sensing pathways of ECs led to the reshaping of endothelial cells and the normalization of tumor blood vessels. Normalization of these vessels dramat-

¹ These authors contributed equally to this work.

² Correspondence: University of Liège, Laboratory of Tumor and Developmental Biology, GIGA-Cancer, Institute of Pathology, CHU-B23, B-4000 Liège, Belgium. E-mail: jmfoidart@ulg.ac.be
doi: 10.1096/fj.09-149070

ically blocked tumor invasion and metastasis and correlated with the up-regulation of vascular endothelial (VE) cadherin and of both VEGF type 1 receptor (VEGFR-1) and its soluble isoform sVEGFR-1. However, the molecular mechanisms integrating these observations remain to be elucidated.

Soluble isoforms of VEGF receptors (VEGFR-1 and -2) named sVEGFR-1 and sVEGFR-2 are detected in blood circulation. These soluble receptors contain the ectodomain of their corresponding full-length isoform and are able to bind their ligands (18–20), thereby controlling their biodisponibility and inhibiting tumor- or ischemia-induced angiogenesis (21–23). The plasma levels of sVEGFR-1 become elevated in pregnant women destined to become preeclamptic later in gestation (24, 25), while those of sVEGFR-2 are increased in leukemic patients and decreased in the presence of an adrenocortical tumor and in systemic lupus erythematosus (26, 27). Moreover, sVEGFR-1 is crucial for proper endothelial sprouting, migration, and branching (28–30). Indeed, the *VEGFR-1*^{−/−} mutant exhibits defects in sprouting and migration that impair vascular branching. This phenotype could be rescued by sVEGFR-1 transgene that also modulates VEGFR-2 signaling.

Altogether, these data suggest that the molecular mechanisms by which sVEGFR-1 and -2 modulates physiological and pathological angiogenesis is more complex than a simple antiangiogenic effect. In this context, the aim of this study is to understand and characterize the potential role of sVEGFR-1 and sVEGFR-2 in vascular maturation, by identifying their implication in interactions between endothelial and mural cells. We report that, during angiogenesis, besides their role of VEGF inhibitors, sVEGFR-1 and sVEGFR-2 are involved in a dialogue between ECs and mural cells, leading to mural cell migration and vascular maturation. Our data provide new insights into molecular mechanisms regulating physiological and pathological angiogenesis and vessel normalization.

MATERIALS AND METHODS

Cell culture and animals

Human umbilical endothelial cells (HUVECs) were isolated as described previously (31). Clonetics human aortic smooth muscle cells (AoSMCs) were purchased from Lonza (Verviers, Belgium). Both primary cells were used from passages 3–8. C57BL/6 and eNOS KO (eNOS^{−/−}) mice (8–12 wk old) were obtained from Charles River Laboratories (L'Arbresle, France). Housing and all animal studies were approved by the ethical committee for the care of experimental animals of the University of Liège (Belgium).

Reagents

Recombinant VEGF was obtained from Peprtech Inc. (London, UK). Recombinant PDGF-BB, sVEGFR-1, sVEGFR-2, sVEGFR-3, Fc of IgG1, sVEGFR-2-specific antibody, and SIP1-specific antibody 1 (MAB2016) were purchased from R&D

Systems (Abingdon, UK). SIP1-specific antibody 2 (sc-25489) was obtained from Santa Cruz Biotechnology (Santa Cruz, CA, USA). SIP1 antagonist VPC 23019 was purchased from Avanti Polar Lipids (Alabaster, AL, USA), protein kinase C (PKC) inhibitor GF109203X from Biomol (Plymouth, PA, USA), and VEGFR-2 tyrosine kinase inhibitor ZM323881 from Tocris Bioscience (Ellisville, MI, USA). *N*-nitro-L-arginine-methyl-ester (L-NAME), *N*-nitro-D-arginine-methyl-ester (D-NAME), 1400W, and 12-myristate 13-acetate phorbol ester (PMA) were obtained from Sigma (St. Louis, MO, USA).

Aortic ring assay, whole-mount immunostaining, and quantification

Mouse aortic rings were cultured in 3-D collagen gels as described previously (32). Effects of recombinant VEGF, sVEGFR-1 or -2, and ZM323881 were evaluated after 9 d of incubation on aortic rings. A modified assay consisted of incubated the rings with VEGF over 5 d, then media were supplemented or not with sVEGFR-1 or -2 for 1 d. Quantifications of cellular network outgrowth were performed using image analysis algorithms with the software Aphelion 3.2 (Adcis, Hérouville Saint-Clair, France) (33). At the end of cultures, aortic fragments embedded in collagen gels fixed in 4% paraformaldehyde and blocked with 1.5% milk were immunolabeled with primary lectins or antibodies: *Griffonia simplicifolia* isolectin-B4/Alexa Fluor 488 (IB4, 121411; Invitrogen Molecular Probes, Merelbeke, Belgium), rabbit anti-NG2 chondroitin sulfate proteoglycan (NG2, AB5320; Millipore-Chemicon, Brussels, Belgium), then with a secondary rabbit-IgG-specific biotinylated antibody (E432; DakoCytomation, Glostrup, Denmark), and finally mounted with Vectashield-DAPI mounting medium (H-1200; Vector Laboratories, Burlingame, CA, USA).

FITC staining and receptor binding assay in cell-free condition

Recombinant sVEGFR-1/Fc and sVEGFR-2/Fc were conjugated with fluorescein isothiocyanate (FITC) using Fluorescein Protein Labeling Kit (1 386 093; Roche, Mannheim, Germany) according to the manufacturer's instructions. Then a 96-wells microplate was coated with VEGF (2 µg/ml) or with vehicle (NaHCO₃, pH 8.4), saturated with PBS containing 1% BSA, then incubated with various dilutions of FITC-conjugated sVEGFR-2. Bound sVEGFR-2 was evidenced using an anti-FITC-HRP linked antibody (16 848 17; Roche), and the reaction was revealed with TMB solution [0.42 mM TMB, 0.004% H₂O (v/v), in 100 mM sodium acetate/citric acid, pH 4.9]. The reaction was stopped by addition of H₂SO₄ (0.9 M). Assay absorbency was measured using an automatic spectrophotometer (Multiskan MS; Labsystems, Vantaa, Finland) at 450 vs. 620 nm.

VEGF and VEGFR-2 screening

HUVECs and AoSMCs were cultured in serum-free media during 24 h. Then media were collected and cells were lysed in order to isolate either proteins or ARN. VEGF was quantified in media according to the manufacturer's instructions by DuoSet ELISA (DY293B; R&D Systems). Western blot was performed using the following antibodies: VEGF-specific antibody (sc-152; Santa Cruz Biotechnology), VEGFR2-specific antibody (2479; Cell Signaling Technology, Danvers, MA, USA), and rabbit-IgG-specific HRP-linked antibody (7074; Cell Signaling Technology). RT-PCRs were run with the following primers: VEGF (forward) 5'-CC-TGGTGGACATCTTCCAGGAGTA-3', (reverse) 5'-CTCA-

CCGCCTCGGCTTGTCACA-3'; VEGFR-2 (forward) 5'-TT-CCACGTGACCAGGGGTCT-3', (reverse) 5'-AGCTG-CCTGACCACGCAATGT-3'. RT-PCR products were quantified by normalization with respect to 28S ribosomal RNA.

Cell proliferation assay

The effect of VEGF, sVEGFR-1 or -2, used alone or mixed on HUVEC and AoSMC proliferation, was quantified after 24, 48, or 72 h by BrdU incorporation into DNA with a colorimetric cell proliferation ELISA kit (11 647 229 001, Roche) according to the manufacturer's instructions. In some experiments, culture medium was replaced by HUVEC-conditioned medium. For HUVEC medium conditioning, see below.

Modified Boyden chamber migration assay

For HUVEC and AoSMC migration assay, polycarbonate filters (8- μ m pore) of Transwell Permeable Support (Costar; Corning, Lowell, MA, USA) were treated overnight at room temperature with 0.005% gelatin. Cells were suspended in serum-free medium containing 0.1% BSA and placed on the upper compartment of the chamber (10⁵ cells/filter). The lower compartment of the chamber was filled with medium containing 1% FCS and 1% BSA, supplemented with or without VEGF, sVEGFR-1, or -2. In some experiments, the lower compartment of the chamber was filled with HUVEC-conditioned medium prepared as described in the HUVEC medium conditioning section.

AoSMC migration was also evaluated in coculture with HUVECs. For this, HUVECs were seeded in the lower compartment of the Transwell coated with gelatin and filled with medium containing 1% FCS and 1% BSA, supplemented with the tested reagents. AoSMCs were seeded in the upper compartment of the chamber as described above. After an incubation at 37°C for periods of 12, 24, and 48 h, filters were fixed in methanol and media were collected, centrifuged (10,000 g, 15 min, 4°C), then stored at -20°C until ELISA was performed. Cells on filters were stained with 0.1% crystal violet solution (Sigma). Nonmigrated cells at the upper surface of the filters were wiped away with a cotton swab. Quantification of the migration assay was done by colorimetric measurement (λ =560 nm) resulting from cells having migrated at the lower surface of the filter. The following factors were measured, in media of the lower chamber, by ELISA, according to the manufacturer's instructions: PDGF-BB (DY220; R&D Systems) Ang1 (DY923; R&D Systems), bFGF (DY233; R&D Systems), TGF- β 1 (DY240; R&D Systems), and S1P (K-1900; Echelon Biosciences, Salt Lake City, UT, USA).

Cord-like structure formation assay and quantification in Matrigel

A cocultured 3-D model of cord-like formation in Matrigel was used to define mural cell organization around EC cord-like structures. Briefly, HUVECs stained with CellTracker-CMFDA dye (green, C2925; Invitrogen Molecular Probes, Merelbeke, Belgium) were seeded on Matrigel and allowed to form cord-like structures by 6 h of incubation. Then AoSMCs stained with CellTracker-CMRA dye (orange, C34551; Invitrogen Molecular Probes) were seeded over EC cords simultaneously with drugs. Analysis of the AoSMC distribution around the EC cord network was computer-assisted quantified by implementing an algorithm using the image analysis toolbox of MATLAB 7.1 software (MathWorks, Natick, MA, USA). This method calculated the smallest distance present between neighboring green pixel corresponding to ECs and orange pixel corresponding to AoSMCs.

In vivo mouse Matrigel plug assay, immunostaining, and quantification

The mouse Matrigel plug assay was performed as described previously (34). Briefly, Matrigel (500 μ l) was injected subcutaneously into both flanks of C57BL/6 mice. Matrigel containing heparin (10 U/ml) was supplemented or not with VEGF (250 ng/ml), sVEGFR-1, or sVEGFR-2 (2 μ g/ml). After 10 d, plugs were collected either for hemoglobin (Hb) quantification, or for subsequent immunostaining. Hb quantification was performed as described previously (31). For immunostaining, fluorescein isothiocyanate (FITC)-conjugated dextran was perfused for 5 min before mice were sacrificed. Matrigel plugs were collected, embedded in Tissue-Tek, and stored at -80°C. For immunostaining, thick sections (100 μ m) were cut, fixed for 10 min in 4% PFA, then immunolabeled with Cy3-conjugated anti- α smooth muscle actin (SMA) antibody (C6198; Sigma) and mounted with Vectashield-DAPI mounting medium. To evaluate the localization of mural cells, pictures were recorded using a Leica TCS SP2 confocal microscope (Leica Microsystems, Wetzlar, Germany). Analysis of the density of vessels covered by mural cells was quantified by implementing an algorithm using the image analysis toolbox of MATLAB7.1 software (MathWorks). For this analysis, 1-4 optical fields/plug section (\times 10 or \times 20) were randomly chosen and recorded using an Olympus AH-3 microscope (Olympus, Aarstelaar, Belgium). Images were registered in the RGB color space, and color images were split into their 3 components. Each green and red picture was binarized using an automatic threshold in order to determine the total area of vessel and mural cells, respectively. Then the area of intersected region, occupied by both vessels and mural cells, was determined. Colocalization density was defined as the area of this intersected region divided by total area occupied by vessels.

HUVEC medium conditioning

HUVECs in stock culture were replated in 6-cm culture dishes and cultured in 2 ml of basal medium (culture medium supplemented with 1% FCS and 1% BSA) supplemented or not with VEGF (50 ng/ml), sVEGFR-1 (250 ng/ml), or sVEGFR-2 (250 ng/ml). After 4, 24, or 48 h of incubation, media were collected, centrifuged (10,000 g, 15 min, 4°C) and stored at -20°C until ELISA was performed or until they were used for BrdU uptake or Boyden chamber migration assays. The following factors were measured by ELISA, according to the manufacturer's instructions: PDGF-BB (DY220; R&D Systems) Ang1 (DY923; R&D Systems), bFGF (DY233; R&D Systems), TGF- β 1 (DY240; R&D Systems), S1P (K-1900; Echelon Biosciences).

Western blot and ERK1/2 phosphorylation analysis

For phosphorylated VEGFR-2 (phospho-VEGFR-2), phosphorylated eNOS (phospho-eNOS) and S1P1 detection by Western blot 15 μ g of whole-cell extracts were resolved on 8 or 10% SDS-PAGE after cells had been incubated with PDGF-BB, sVEGFR-1, sVEGFR-2, or vehicle (serum-free medium) for 10 min to 24 h. Protein loading was controlled by glyceraldehyde-3-phosphate dehydrogenase (GAPDH) immunodetection. Antibodies used at concentration recommended by the manufacturer were phospho-VEGFR-2 (Tyr1175)-specific antibody (2478; Cell Signaling Technology), phospho-eNOS (Ser-1177)-specific antibody (9571; Cell Signaling Technology), SP1-specific (EDG-1) antibody (MAB2016; R&D Systems), GAPDH-specific anti-

body (MAB374; Millipore-Chemicon), mouse-IgG-specific HRP-linked antibody (7076; Cell Signaling Technology), and rabbit-IgG-specific HRP-linked antibody (7074; Cell Signaling Technology). Immunocomplexes were visualized by chemiluminescence reaction on a luminescent image analyzer (LAS-4000; Fujifilm, Wavre, Belgium). Intensity of bands was quantified using Quantity-One software (Bio-Rad Laboratories, Nazareth Eke, Belgium) and normalized with respect to GAPDH expression.

Phosphorylation of ERK1/2 was quantified by DuoSet IC ELISA DYK1018 (R&D Systems) according to the manufacturer's instructions.

Binding of sVEGFR-1/FITC and -2/FITC to EC

HUVECs were cultured in 24-well plates or on a coverslip with vehicle or with sVEGFR-1/FITC or sVEGFR-2/FITC mixed with VEGF (0.5 ng/ml) for 2 h at 4°C. After cross-linking, cells were either lysed for subsequent Western blot analysis, either fixed for 10 min in 4% PFA for subsequent immunocytochemistry analysis. Western blot was performed using a FITC-specific HRP-linked antibody (16 848 17, Roche). Protein loading was controlled by GAPDH immunodetection. Immunocomplexes were visualized by chemiluminescence reaction on a luminescent image analyzer (LAS-4000, Fujifilm, Wavre, Belgium). Immunocytochemistry was conducted with a FITC-specific alexa488-linked antibody (A11090; Invitrogen Molecular Probes), and cells were mounted with Vectashield-DAPI mounting medium. Photomicrographs were recorded using an Olympus AH-3 microscope.

S1P1 RT-PCR

HUVECs were preincubated or not for 15 min with the PKC inhibitor GF109203X. Then cells were incubated with vehicle or with PMA, VEGF, sVEGFR-1, or sVEGFR-2 for 60 min to 4 h before total RNA was extracted with the kit RNeasy (Qiagen, Valencia, CA, USA), according to the manufacturer's protocol. S1P1 mRNAs were measured with the following primers: S1P1 (forward) 5'-GCCCACTGGTTTCTGCGGAA-3', (reverse) 5'-ACCAAGGAGTAGATCCTGCAGTA-3'. S1P1 products were quantified by normalization with respect to 28S ribosomal RNA.

Statistical analysis

All quantitation experiment data are expressed as means \pm SD or means \pm SE. Statistical analyses were conducted with GraphPad Prism software (GraphPad, La Jolla, CA, USA) using 1-way ANOVA followed by Student-Newman-Keuls's test or using Kruskal-Wallis followed by Dunn's test, with regard to heteroscedasticity. For computerized image analysis, statistical analysis were performed with the statistics toolbox of MATLAB 7.1 (MathWorks) using Student's *t* test or Wilcoxon test, with regard to heteroscedasticity. Values of $P \leq 0.05$ were considered as statistically significant.

RESULTS

sVEGFR-1 and -2 promote mural cell network outgrowth in aortic ring assay

VEGF, but also, unexpectedly, the antiangiogenic sVEGFR-1 or -2, stimulated the outgrowth of a cellular

network from the aortic ring (**Fig. 1A**) that was quantified by computer-assisted image analysis (**Fig. 1B**). Immunostaining of whole-mount aortic ring explants cultured in the presence of VEGF identified vessel outgrowth as composed of isolectin-B4 (IB4) -positive ECs (**Fig. 1C**). However, in the absence of exogenous VEGF, addition of sVEGFR-1 or -2 promoted the outgrowth of an IB4-negative, but NG2 chondroitin sulfate proteoglycan (NG2) -positive (identifying mural cells) cellular network. In this model, isolated round IB4 positive cells were leukocytes. In addition, when the aortic rings were first incubated with VEGF then supplemented with sVEGFR-2 (**Fig. 1D**), a visible increase of NG2-positive cells covering endothelial vessels was induced.

The VEGF-neutralizing effect of the chimeric recombinant sVEGFR-1/Fc and sVEGFR-2/Fc, used in our experimental conditions, was assessed with a receptor-binding assay in cell-free conditions (**Fig. 2A**) and by measurement of free VEGF in media supplemented with these soluble receptor recombinant proteins (**Fig. 3D**). Both sVEGFR-1/Fc and -2/Fc inhibited VEGF-driven effect on endothelial cell proliferation and migration (**Fig. 2C, D**), as well as in the *ex vivo* aortic ring assay (**Fig. 2E**) and, finally, by the *in vivo* matrigel plug assay (**Fig. 2F**). ERK1/2 phosphorylation was also evaluated (**Fig. 2B**) in the presence of VEGF, and a decrease of this VEGF-induced phosphorylation was observed when sVEGFR-1 or -2 was added. Collectively, these results confirm that both recombinant sVEGFRs/Fc possess the ability to bind VEGF and inhibit VEGF-dependent endothelial cell angiogenesis. The soluble VEGF receptors did not directly modulate EC differentiation, proliferation, or migration, but primarily affected EC activities by neutralizing VEGF. sVEGFR-1 and -2 modulated angiogenesis not only by inhibiting VEGF action, but also by promoting the outgrowth of mural cells.

sVEGFR-1 and -2 promote vessel stabilization *in vitro* and *in vivo*

We evaluated the impact of sVEGFR-1 and -2 on the codistribution of mural cells and ECs in a 3-D model of cord-like formation in Matrigel (**Fig. 4A**). EC cords were preformed before the addition of mural cells. Interestingly, perivascular cell distribution calculated as a distance away from EC cords showed that the density of mural cells closely opposed to the EC cords (distance $\leq 5 \mu\text{m}$) was 2-fold higher under sVEGFR-1 or -2 treatments. Reciprocally, the density of mural cells distant from EC cords by $75 \mu\text{m}$ was 1.5-fold lower on sVEGFRs treatment (**Fig. 4B**). The mean distance between mural cells and EC cords was significantly reduced by 40% in the presence of either sVEGFR. Moreover, in the aortic ring assay, the addition of sVEGFR-1 or -2 after 5 d of VEGF treatment increased the coverage by mural cells of the endothelial cords (data not shown).

To investigate *in vivo* the impact of both sVEGFRs on mural cell recruitment, we examined mural cell coverage of neovessels formed in Matrigel plugs subcutaneously injected to C57BL/6 mice. Perfused vessels were visualized through intravenous injection of FITC-conjugated dextran. Mural cells were immunostained with

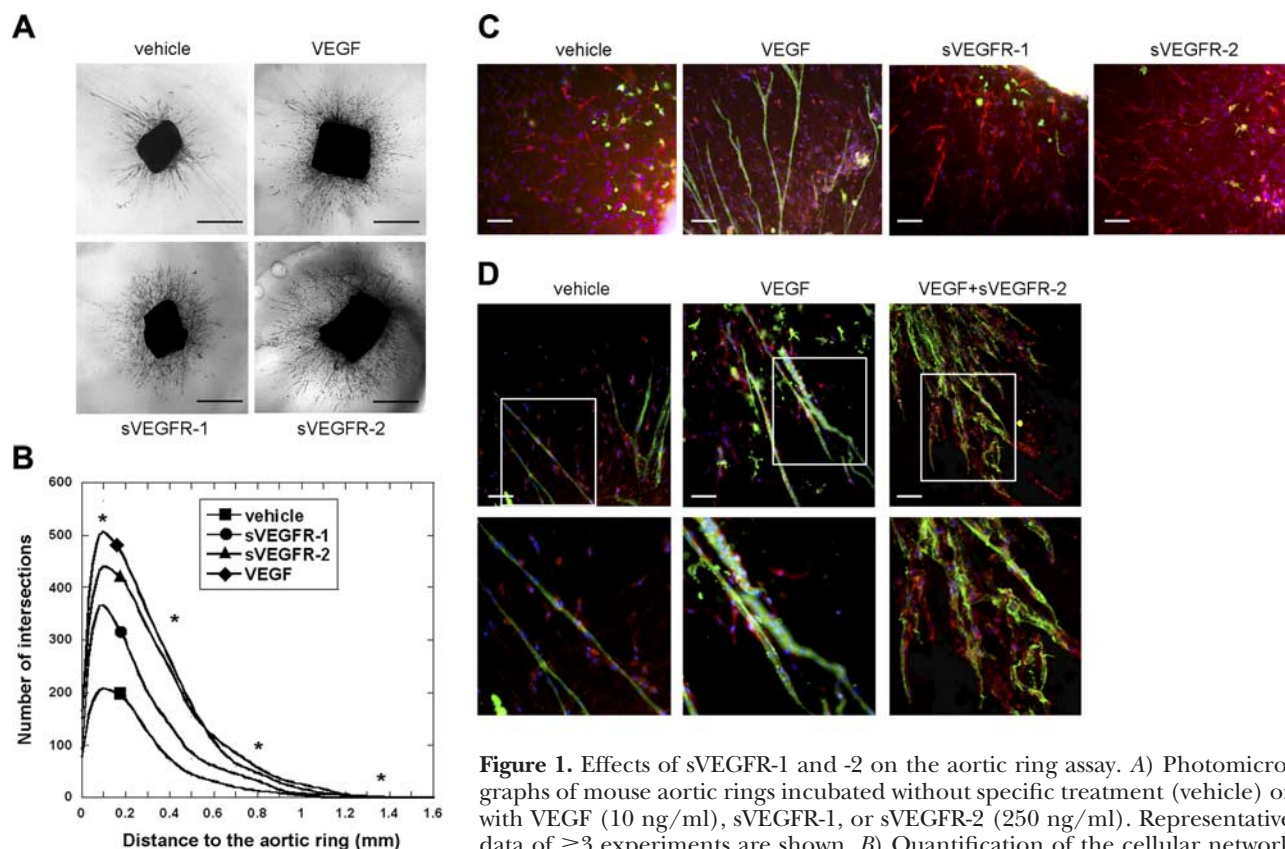


Figure 1. Effects of sVEGFR-1 and -2 on the aortic ring assay. **A)** Photomicrographs of mouse aortic rings incubated without specific treatment (vehicle) or with VEGF (10 ng/ml), sVEGFR-1, or sVEGFR-2 (250 ng/ml). Representative data of ≥ 3 experiments are shown. **B)** Quantification of the cellular network outgrowing from mouse aortic ring. Each curve is a mean of the cellular network distribution obtained by the average of ≥ 5 individual distributions generated for each experimental condition. Mouse aortic rings were incubated without specific treatment (vehicle) or with VEGF (10 ng/ml), sVEGFR-1, or sVEGFR-2 (250 ng/ml) treatments. $*P < 0.05$. Representative data of ≥ 3 experiments are shown. **C)** Photomicrographs of mouse aortic ring immunostained with IB4-specific antibody (IB4, green) identifying ECs and with NG2-specific antibody (NG2, red) identifying PC/SMCs. Nuclei were stained with DAPI (blue). Aortic rings were incubated without specific treatment (vehicle) or with VEGF (10 ng/ml), sVEGFR-1, or sVEGFR-2 (250 ng/ml). Representative data of ≥ 3 experiments are shown. **D)** Photomicrographs of mouse aortic ring immunostained with IB4-specific antibody (IB4, green) identifying ECs and with NG2-specific antibody (NG2, red) identifying PC/SMCs. Nuclei were stained with DAPI (blue). Aortic rings were incubated without specific treatment (vehicle) or with VEGF (10 ng/ml) for 5 d, then media were supplemented or not with sVEGFR-2 (250 ng/ml). Scale bars = 1 mm (A); 100 μ m (C, D).

Cy3-conjugated α -SMA antibody. Staining with this mural cell marker revealed an increase of mural cell coverage when the Matrigel plug was supplemented with sVEGFR-1 (Fig. 4C). The quantification by computer-assisted image analysis showed that the density of vessels covered by mural cells was increased by 63 and 114% under treatment with sVEGFR-1 or PDGF-BB (used as a positive control), respectively (Fig. 4D). For each experimental condition, confocal microscopy analysis attested that α -SMA positive cells surrounded functional vessels (Fig. 4E). Similar data were obtained with sVEGFR-2 (data not shown).

Induction of mural cell migration by sVEGFR-1 and -2 requires EC neighboring

The impact of sVEGFR-1 and -2 was evaluated on mural cell migration (Fig. 5A) and proliferation (Fig. 5B) using PDGF-BB as positive control. Neither VEGF nor sVEGFR treatments modified aortic smooth muscle cell migration or proliferation after 12, 24, 48, or 72 h exposure,

indicating that VEGF or sVEGFRs have no direct effect on mural cell proliferation and migration.

We next evaluated the influence of these sVEGFRs on AoSMC migration when cocultured with HUVECs in a modified Boyden chamber assay. After 12, 24, or 48 h of incubation, AoSMC migration was stimulated not only by PDGF-BB treatment, but also in a dose-dependent way on sVEGFR-1 or -2 exposure (Fig. 5C). The effect of PDGF-BB persisted in the absence of HUVECs, showing a direct effect of this cytokine on AoSMC migration. On the other hand, the presence of HUVECs was required to observe an increase in AoSMC migration in the presence of sVEGFR-1 or -2. As the recombinant sVEGFR-1 and -2 used in this work were chimeric proteins fused to the Fc region of human IgG1, we verified the specificity of their effect, by demonstrating an absence of regulation of AoSMC migration by the same Fc region of IgG1 alone (2–250 ng/ml) and by another chimeric recombinant protein of the VEGF family, sVEGFR-3, fused to the same Fc region (Fig. 5C).

After 12 or 24 h of incubation, we observed that a

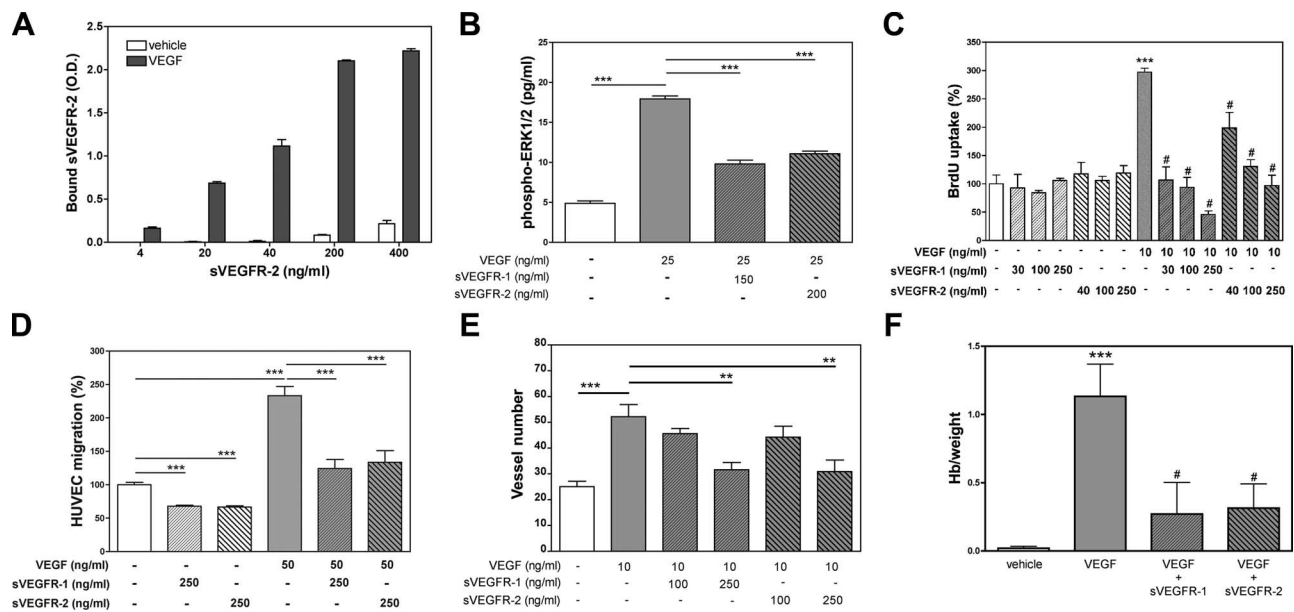


Figure 2. Anti-VEGF activity of sVEGFR-1/Fc and sVEGFR-2/Fc. **A)** Histogram of receptor binding assay to VEGF in cell-free conditions. Results are expressed as optical density (O.D.) of sVEGFR-2 bound to plate wells coated with VEGF or vehicle, means \pm SD, $n = 4$. **B)** Histogram of ERK1/2 phosphorylation in HUVECs obtained after 10 min of incubation. For specific treatments see the figure. Results (means \pm SE) show the concentration (pg/ml) of phosphorylated ERK1/2 of 6 independent experiments run in triplicate. *** $P < 0.001$. **C)** Histogram of HUVEC growth after 48 h under treatment. For specific treatments see the figure. Results are expressed as percentage of BrdU uptake, means \pm SD, $n = 5$. *** $P < 0.001$ vs. vehicle; # $P < 0.001$ vs. VEGF treatment. Representative data of 3 independent experiments are shown. **D)** Histogram of HUVEC migration after 10 h under treatment. For specific treatments see the figure. Results (means \pm SD) show the percentage of HUVEC migration of 3 independent experiments run in triplicate. *** $P < 0.001$ vs. vehicle. **E)** Histogram of vessel number outgrowing from mouse aortic rings. For specific treatments see the figure. Results are means \pm SE, $n = 8$. ** $P < 0.01$; *** $P < 0.001$. **F)** Histogram of Hb matrigel plug content reported to plug weight. Matrigel was supplemented without specific treatment (vehicle) or with VEGF (250 ng/ml) and sVEGFR-1 or -2 (2 μ g/ml). Results are means \pm SE, $n = 8$. *** $P < 0.001$ vs. vehicle, # $P < 0.01$ vs. VEGF.

neutralizing sVEGFR-2-specific antibody inhibited the promigratory effect induced by sVEGFR-2 (Fig. 5D), with a maximal neutralizing effect when used in a ratio of 5:1 (anti-sVEGFR-2 vs. sVEGFR-2).

In our experimental conditions, VEGF is expressed at

the mRNA and protein levels by HUVECs. However, the protein is not secreted at a detectable level in the medium conditioned by HUVECs (Fig. 3). On the other hand, the AoSMCs produce and secrete VEGF. Note that the level of intracellular VEGF protein is

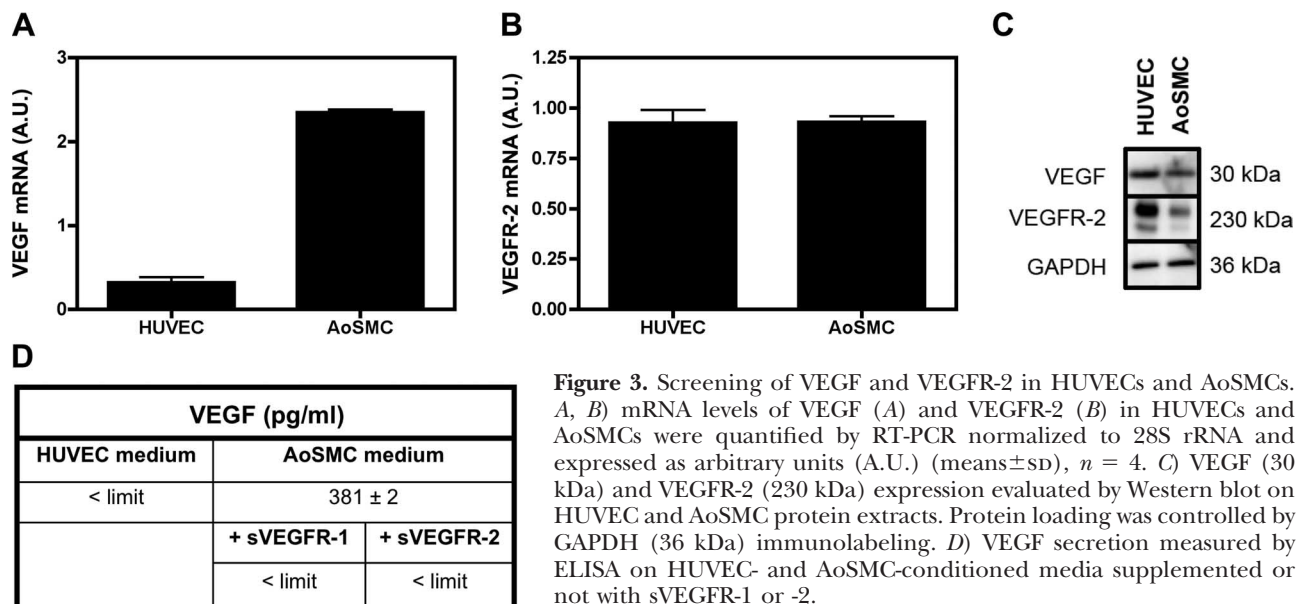


Figure 3. Screening of VEGF and VEGFR-2 in HUVECs and AoSMCs. **A, B)** mRNA levels of VEGF (**A**) and VEGFR-2 (**B**) in HUVECs and AoSMCs were quantified by RT-PCR normalized to 28S rRNA and expressed as arbitrary units (A.U.) (means \pm SD), $n = 4$. **C)** VEGF (30 kDa) and VEGFR-2 (230 kDa) expression evaluated by Western blot on HUVEC and AoSMC protein extracts. Protein loading was controlled by GAPDH (36 kDa) immunolabeling. **D)** VEGF secretion measured by ELISA on HUVEC- and AoSMC-conditioned media supplemented or not with sVEGFR-1 or -2.

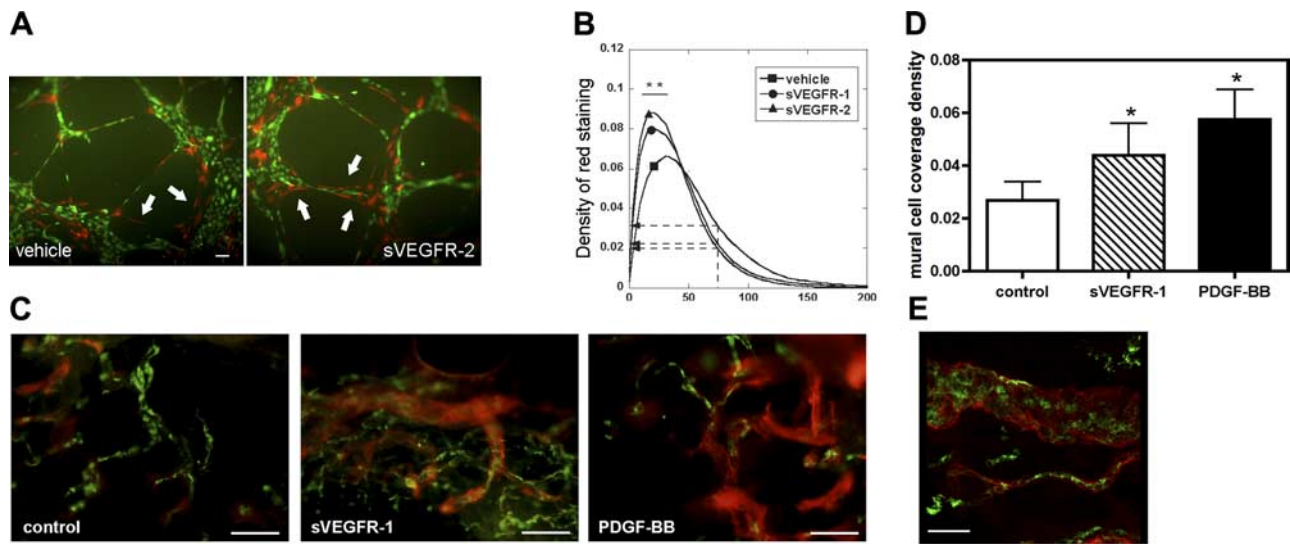


Figure 4. Effect of sVEGFR-1 and -2 on PC/SMC recruitment. *A*) Photomicrographs of 3-D cord-like structure obtained from HUVECs (green staining) cocultured with AoSMCs (orange staining) on Matrigel and incubated without specific treatment (vehicle) or with sVEGFR-2 (250 ng/ml). Arrows indicate area where AoSMCs are distant from or close to endothelial cord-like structure. Representative data of ≥ 3 experiments are shown. *B*) AoSMC distribution around a HUVEC cord network. Each curve is a mean of AoSMC distribution obtained by the average of ≥ 5 individual distributions generated for each experimental condition. Cocultures of HUVECs and AoSMCs were incubated without specific treatment (vehicle) or under sVEGFR-1 or sVEGFR-2 (250 ng/ml) treatments. $**P < 0.05$. Representative data of ≥ 3 experiments are shown. *C*) Photomicrographs of vessels grown in Matrigel supplemented without specific treatment (control) or with sVEGFR-1 (2 μ g/ml) or PDGF-BB (250 ng/ml). Vessels are visualized by FITC-conjugated dextran (green) perfusion, mural cells are stained by α -SMA immunostaining (red). *D*) Quantification of mural cell coverage density. Results (means \pm SE, $n = 12$ animals/group) show the mural cell coverage density resulting from the ratio between the area of vessel covered by mural cells and the total vessel area. $*P \leq 0.05$. *E*) Representative photomicrograph obtained by confocal microscopy showing that mural cells cover functional vessels. Vessels are visualized by FITC-conjugated dextran (green) perfusion, mural cells are stained by α -SMA immunostaining (red). Scale bars = 100 μ m (*A*, *C*); 30 μ m (*E*).

lower in AoSMCs than in HUVECs. These results reveal that in HUVECs, the majority of VEGF produced remains inside the cells, while VEGF produced by AoSMCs is secreted in the extracellular milieu. Moreover, AoSMCs expressed VEGFR-2, albeit at a lesser extent than in HUVECs.

sVEGFR-1 and -2 promote mural cell migration through EC eNOS activation

To determine whether the indirect promigratory effect of sVEGFR-1 and -2 could be mediated by a stable factor secreted by ECs under sVEGFR-1 or -2 treatment, AoSMC

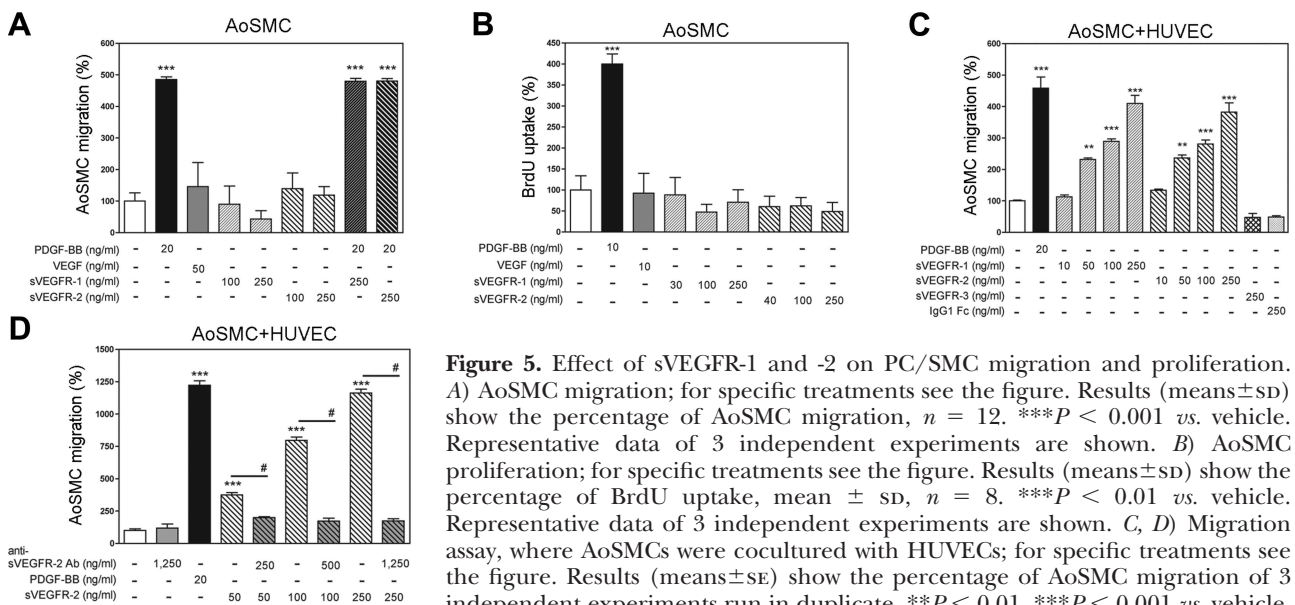


Figure 5. Effect of sVEGFR-1 and -2 on PC/SMC migration and proliferation. *A*) AoSMC migration; for specific treatments see the figure. Results (means \pm SD) show the percentage of AoSMC migration, $n = 12$. $***P < 0.001$ vs. vehicle. Representative data of 3 independent experiments are shown. *B*) AoSMC proliferation; for specific treatments see the figure. Results (means \pm SD) show the percentage of BrdU uptake, mean \pm SD, $n = 8$. $***P < 0.01$ vs. vehicle. Representative data of 3 independent experiments are shown. *C*, *D*) Migration assay, where AoSMCs were cocultured with HUVECs; for specific treatments see the figure. Results (means \pm SE) show the percentage of AoSMC migration of 3 independent experiments run in duplicate. $**P < 0.01$, $***P < 0.001$ vs. vehicle, $\#P < 0.001$ vs. sVEGFR-2.

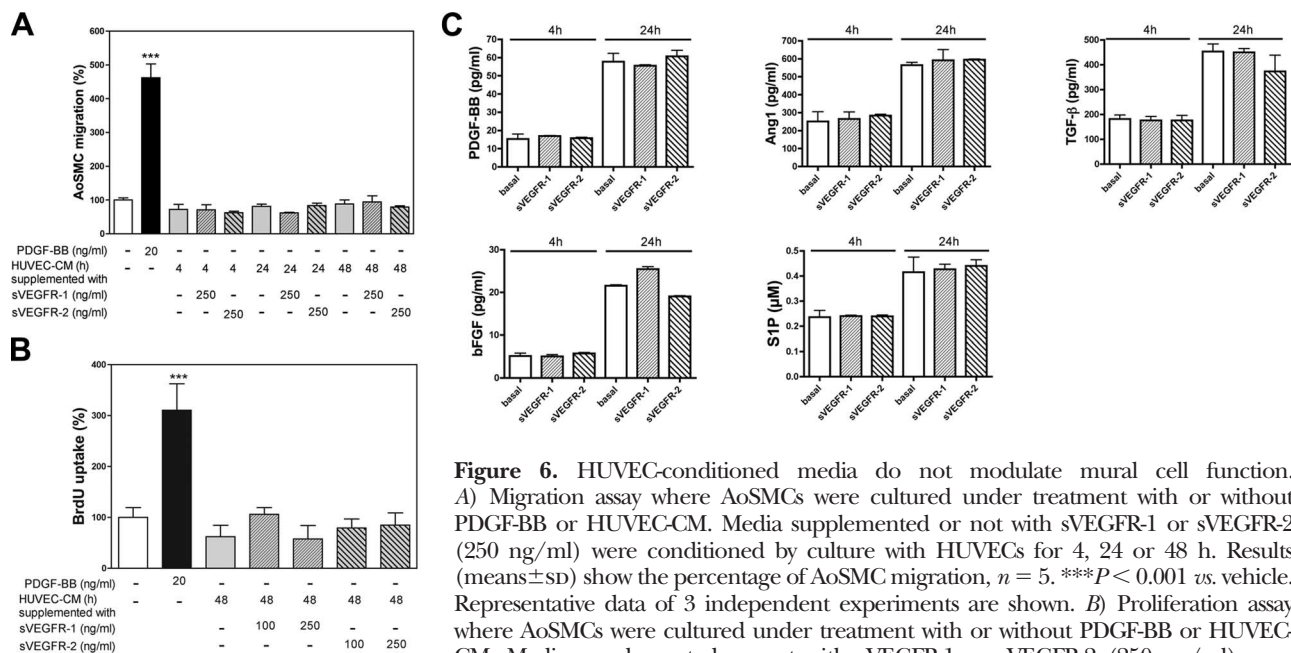


Figure 6. HUVEC-conditioned media do not modulate mural cell function. **A)** Migration assay where AoSMCs were cultured under treatment with or without PDGF-BB or HUVEC-CM. Media supplemented or not with sVEGFR-1 or sVEGFR-2 (250 ng/ml) were conditioned by culture with HUVECs for 4, 24 or 48 h. Results (means \pm SD) show the percentage of AoSMC migration, $n = 5$. *** $P < 0.001$ vs. vehicle. Representative data of 3 independent experiments are shown. **B)** Proliferation assay where AoSMCs were cultured under treatment with or without PDGF-BB or HUVEC-CM. Media supplemented or not with sVEGFR-1 or sVEGFR-2 (250 ng/ml) were conditioned by culture with HUVECs for 48 h. Results (means \pm SD) show the percentage of BrdU uptake, $n = 8$. *** $P < 0.001$ vs. vehicle. Representative data of 3 independent experiments are shown. **C)** ELISA of PDGF-BB, Ang1, TGF- β , bFGF, and S1P performed on media supplemented or not with sVEGFR-1 or sVEGFR-2 (250 ng/ml) and conditioned by culture with HUVECs for 4 or 24 h. Results are means \pm SD, $n = 5$.

migration was tested in the presence of medium conditioned by HUVECs previously cultivated with or without sVEGFR-1 or -2 for 4, 24, or 48 h (Fig. 6A). In sharp contrast to what was observed when AoSMCs were cocultured with HUVECs, HUVEC-conditioned media (HUVEC-CM) previously supplemented with sVEGFR-1 or -2 failed to induce AoSMC migration after 12, 24, or 48 h exposure. In addition, none of the HUVEC-CM tested was able to stimulate AoSMC proliferation even after 24–72 h (Fig. 6B). Levels of cytokines known to stimulate AoSMC migration (PDGF-BB, Ang1, TGF- β , bFGF, and S1P) in HUVEC-CM and in media of cocultured Boyden chamber assay were identical in basal or sVEGFRs supplemented conditions (Fig. 6C). Altogether, these results demonstrate that the treatment of HUVECs with sVEGFR-1 or sVEGFR-2 did not increase the secretion of any stable factor that could modulate migration or proliferation of AoSMCs.

Hence, we hypothesized that the promigratory effect of sVEGFR-1 and -2 on AoSMCs could be due to a volatile factor such as NO, which is known to stimulate PC recruitment (14, 35, 36). L-NAME, a pan-inhibitor of NOS, did not modulate basal and PDGF-BB-induced AoSMC migration, but completely inhibited the promigratory effect induced by sVEGFR-1 and -2 in the modified Boyden chamber assay (Fig. 7A). L-NAME also decreased the cellular network outgrowth induced by sVEGFR-2 (Fig. 7B) in the aortic ring assay. By immunostaining, the cellular network outgrowth was identified as being composed mainly of PC/SMCs (data not shown). Computer-assisted image analysis quantification confirmed that L-NAME reduced the mural cell outgrowth induced by sVEGFR-2 treatment (Fig. 7C). Similar results were obtained with sVEGFR-1 (data not

shown). On the other hand, D-NAME, the inactive isomer of L-NAME, and 1400W, a selective inhibitor of inducible NOS (iNOS), did not inhibit the promigratory effect by sVEGFR-1 and -2. Since neuronal NOS (nNOS) is not expressed by HUVECs, these data indicate that eNOS activity is involved in this promigratory process. In addition, the outgrowth of the mural cell network promoted by sVEGFR-1 and -2 in wild-type (WT) mouse aorta rings was completely inhibited with eNOS^{-/-} mouse aorta (Fig. 7D). Collectively, these results demonstrate that eNOS activity is involved in the recruitment of mural cells induced by sVEGFR-1 and -2.

EC S1P1 is involved in the process by which sVEGFR-1 and -2 modulate PC/SMC function

On the basis of its ability to trigger eNOS activation and NO synthesis by ECs and regarding its key role in endothelium maturation (15, 37–39), we hypothesized that S1P1 could be involved in sVEGFRs-promoted PC/SMC migration. Treatment of HUVECs with sVEGFR-1 and -2 but not with PDGF-BB led to an accumulation of S1P1, as documented by quantified Western blot (Fig. 8A–B). This overproduction occurred from 60 to 90 min of incubation in the presence of the sVEGFRs and was maintained up to 10 h. In addition, 2 different S1P1-specific antibodies and an S1P1 antagonist (VPC 23019) that does not modulate PDGF-BB-induced AoSMC migration completely inhibited the mural cell promigratory effect observed in the presence of sVEGFR-1 and -2 (Fig. 8C, D). These data strongly support that S1P1 is involved in the para-

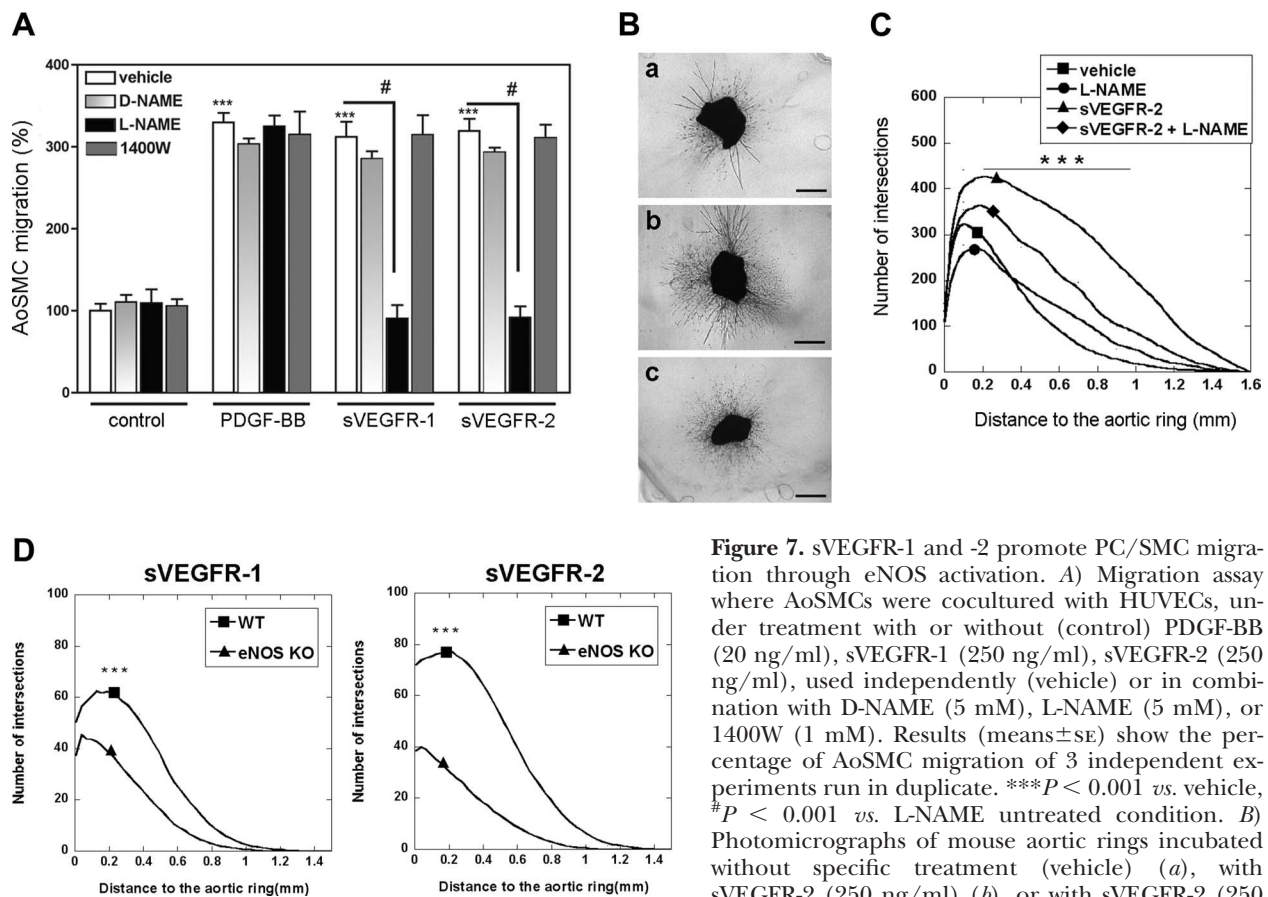


Figure 7. sVEGFR-1 and -2 promote PC/SMC migration through eNOS activation. **A)** Migration assay where AoSMCs were cocultured with HUVECs, under treatment with or without (control) PDGF-BB (20 ng/ml), sVEGFR-1 (250 ng/ml), sVEGFR-2 (250 ng/ml), used independently (vehicle) or in combination with D-NAME (5 mM), L-NAME (5 mM), or 1400W (1 mM). Results (means \pm SE) show the percentage of AoSMC migration of 3 independent experiments run in duplicate. *** P < 0.001 *vs.* vehicle, # P < 0.001 *vs.* L-NAME untreated condition. **B)** Photomicrographs of mouse aortic rings incubated without specific treatment (vehicle) (*a*), with sVEGFR-2 (250 ng/ml) (*b*), or with sVEGFR-2 (250 ng/ml) supplemented with L-NAME (5 mM) (*c*).

Representative data of ≥ 3 experiments are shown. Scale bars = 1 mm. **C)** Quantification of the cellular network outgrowing from mouse aortic ring. Each curve is a mean of the cellular network distribution obtained by the average of ≥ 5 individual distributions generated for each experimental condition. Mouse aortic rings were incubated without specific treatment (vehicle) or with sVEGFR-2 (250 ng/ml) supplemented or not with L-NAME (5 mM). *** P < 0.05. Representative data of ≥ 3 experiments are shown. **D)** Quantification of the cellular network outgrowing from WT or eNOS $^{-/-}$ (eNOS KO) mouse aortic ring. Each curve is a mean of the cellular network distribution obtained by the average of ≥ 5 individual distributions generated for each experimental condition. Mouse aortic rings were incubated with sVEGFR-1 or sVEGFR-2 (250 ng/ml). Representative data of ≥ 3 experiments are shown.

crine interactions leading to mural cell migration under sVEGFRs treatment.

sVEGFR-1 and -2 bind to ECs and modulate VEGFR-2 signaling

To better understand how these soluble VEGF receptor could promote S1P1 up-regulation and eNOS activity, we first evaluated if they could bind to ECs. As shown in **Fig. 9** by immunocytochemistry and by Western blot using FITC-labeled sVEGFR-1 and -2, these soluble VEGF receptors were able to bind HUVECs (**Fig. 9A, B**). sVEGFR-1 and -2 did not completely inhibit the VEGF-induced phosphorylation of VEGFR-2 and of eNOS (**Fig. 9C**), although these soluble receptors, in the same range of concentration, completely trapped free VEGF (**Fig. 3**) and inhibited VEGF-mediated proliferation, migration, differentiation, and angiogenesis (**Fig. 2C–E**). As for PMA and VEGF, both soluble VEGF receptors promoted S1P1 up-regulation through a PKC-dependent pathway (**Fig. 9D**). In the aortic ring

assay, the use of a VEGFR-2 tyrosine kinase inhibitor (ZM323881) did not promote the outgrowth of a mural cell network (**Fig. 9E**).

DISCUSSION

In this study, we identify sVEGFR-1 and sVEGFR-2 as new regulators that contribute to vessel maturation. Our results indicate, as summarized in **Fig. 10**, that sVEGFR-1 and -2 stabilize the immature endothelium through VEGF trapping, interaction with ECs, and the induction of mural cell recruitment. This is mediated in ECs through a paracrine mechanism where sVEGFR-1/-2 and VEGF/VEGFR-2 pathway interplay with the S1P/S1P1 pathway and eNOS activation.

VEGF soluble receptors are 2 physiologically produced VEGF-sequestering proteins that contribute to regulate VEGF isoforms bioavailability in physiological and pathological conditions (24, 40, 41). Even if natural sVEGFR-2 presents a weaker affinity to VEGF than

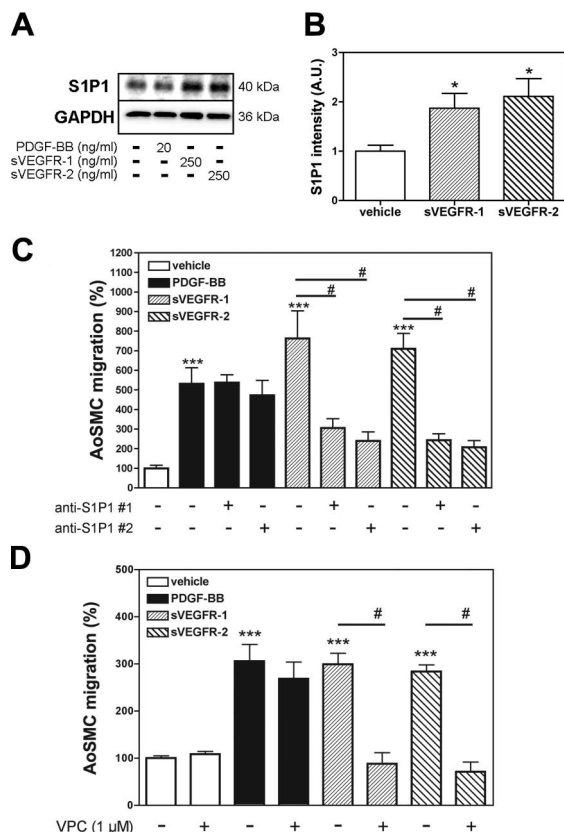


Figure 8. sVEGFR-1 and -2 promote mural cell migration by S1P1 overexpression. **A**) Representative Western blotting of S1P1 (40 kDa) production in HUVECs. Protein loading was controlled by GAPDH (36 kDa) immunolabeling. HUVECs were treated for 60 min; for specific treatments see the figure. **B**) Quantification of S1P1 expression obtained by Western blot. Results (means \pm SE) show the intensity (A.U.) of S1P1 bands of 4 independent experiments run in duplicate. * P < 0.05 *vs.* vehicle. **C**) Migration assay where AoSMCs were cocultured with HUVECs, under treatment with or without PDGF-BB (20 ng/ml), sVEGFR-1 (250 ng/ml), sVEGFR-2 (250 ng/ml), used independently or in combination with an S1P1-specific antibody 1 (1 μ g/ml), another S1P1-specific antibody 2 (1 μ g/ml). Results (means \pm SE) show the percentage of AoSMC migration of 3 independent experiments run in duplicate. *** P < 0.001 *vs.* vehicle, # P < 0.01 *vs.* anti-S1P1 untreated condition. **D**) Migration assay where AoSMCs were cocultured with HUVECs, under treatment with or without PDGF-BB (20 ng/ml), sVEGFR-1 (250 ng/ml), sVEGFR-2 (250 ng/ml), used independently or in combination with VPC 23019 S1P1 antagonist (VPC, 1 μ M). Results (means \pm SE) show the percentage of AoSMC migration of 2 independent experiments run in duplicate. *** P < 0.001 *vs.* vehicle, # P < 0.01 *vs.* VPC untreated condition.

sVEGFR-1 and exhibits an antilymphangiogenic activity in cornea (42, 43), their antiangiogenic activities are well described in different tumoral models (21, 25, 44, 45). However, their potential contribution in vessel stabilization and maturation remained to be explored. In the aortic ring model of angiogenesis, these soluble receptors promoted the outgrowth of a cellular network of mural cells. However, neither endothelial proliferation, migration, and cord-like formation nor PC/SMC proliferation and migration

were directly modulated by sVEGFR-1 or -2. Both sVEGFRs suppressed the bioavailability of VEGF and completely abrogated VEGF-induced EC proliferation, migration, cord-like formation, and angiogenesis *in vitro* and *in vivo*. These results indicate that sVEGFR-1 and -2 can modulate mural cell function in addition to acting at the endothelial level as VEGF trappers. Nevertheless, they failed to exert any direct effect on *in vitro* ECs or mural cell proliferation, migration, and differentiation. These observations led us to speculate that sVEGFR-1 and -2 could recruit mural cells by modulating interactions between neighboring ECs and PC/SMCs. This novel concept is supported by various observations. Indeed, under sVEGFRs treatment, PC/SMCs were attracted toward the endothelial cord-like network in a cocultured 3-D model of cord-like formation and in the aortic ring assay. In addition, we clearly evidenced that sVEGFR-1 and -2, but not sVEGFR-3, a soluble receptor binding VEGF isoforms (VEGF-C, VEGF-D) involved in lymphangiogenesis (33), promoted mural cell migration only in the presence of neighboring ECs. This effect reached the same level as that induced by the PC/SMC promigratory factor PDGF-BB. Moreover, the mural cell coverage of vessels developed, *in vivo*, in a Matrigel plug assay was increased under sVEGFR-1 and -2 treatment. These observations correlate with the study of Mazzone *et al.* (6), who reported an increase of tumor vascular PC coverage associated with an increase of sVEGFR-1 transcription in 3 different tumor models applied to PHD2^{+/-} mice. Altogether, our results sustain that physiological anti-VEGF, sVEGFR-1, is involved in the interaction between ECs and PC/SMCs that promotes the recruitment of mural cells, similarly to what was reported for other inhibitors of the VEGF axis (9, 10, 46). The results obtained with the recombinant sVEGFR-2/Fc reach the same conclusions. However, it must be mentioned that sVEGFR-2/Fc exhibits a higher affinity to VEGF than the physiologically produced sVEGFR-2 (42, 43). Our observations have therefore to be restricted to a therapeutic use of sVEGFR-2/Fc and not completely extrapolated to physiological endogenous interactions.

Recent data suggest that endogenous eNOS-derived NO is involved in arteriogenesis, angiogenesis, and mural cell recruitment (35, 43). Accordingly, in the coculture migration assay and in the aortic ring assay, the pan-NOS inhibitor L-NAME completely inhibited the promigratory effect exerted by sVEGFR-1 and -2 on mural cells. The inability of a selective iNOS inhibitor (1400W) to inhibit sVEGFR-induced PC/SMC migration led us to conclude a selective activation of EC eNOS under sVEGFR treatment. This was confirmed by the loss of effect of these soluble VEGF receptors in an aortic ring assay performed with eNOS^{-/-} mouse aorta. These results are in agreement with the loss of vascular PC coverage observed in an ischemic model performed in eNOS^{-/-} mice (35). In addition, they corroborate the data of Kashiwagi *et al.* (14), who

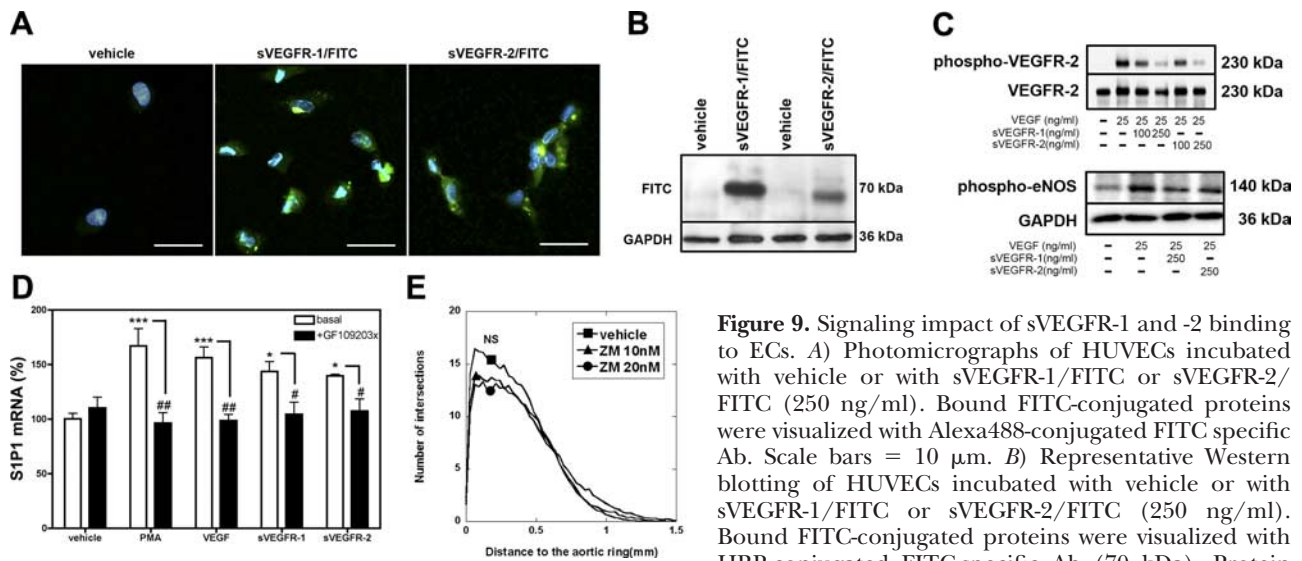


Figure 9. Signaling impact of sVEGFR-1 and -2 binding to ECs. **A)** Photomicrographs of HUVECs incubated with vehicle or with sVEGFR-1/FITC or sVEGFR-2/FITC (250 ng/ml). Bound FITC-conjugated proteins were visualized with Alexa488-conjugated FITC specific Ab. Scale bars = 10 μ m. **B)** Representative Western blotting of HUVECs incubated with vehicle or with sVEGFR-1/FITC or sVEGFR-2/FITC (250 ng/ml). Bound FITC-conjugated proteins were visualized with HRP-conjugated FITC-specific Ab (70 kDa). Protein loading was controlled by GAPDH (36 kDa) immunolabeling. **C)** Phosphorylation of VEGFR-2 (230 kDa)

and of eNOS (140 kDa) was evaluated by Western blot. Protein loading was controlled by GAPDH (36 kDa) or VEGFR-2 (230 kDa) immunolabeling; for specific treatments see the figure. Representative data of ≥ 3 independent experiments are shown. **D)** S1P1 mRNA expression in HUVECs treated with or without PMA (200 ng/ml), VEGF (50 ng/ml), sVEGFR-1 (250 ng/ml), or sVEGFR-2 (250 ng/ml) + VEGF (0.5 ng/ml). Cells were preincubated with vehicle (basal) or with GF109203X. Results (means \pm SE) show the percentage of S1P1 mRNA expression of 2 independent experiments run in duplicate. * $P < 0.05$, *** $P < 0.001$ vs. vehicle; # $P < 0.05$, ## $P < 0.001$ vs. GF109203X untreated condition (basal). **E)** Quantification of the cellular network outgrowing from mouse aortic ring. Each curve is a mean of the cellular network distribution obtained by the average of ≥ 5 individual distributions generated for each experimental condition. Mouse aortic rings were incubated without specific treatment (vehicle) or with ZM323881 (ZM); NS, not significant. Representative data of ≥ 3 experiments are shown.

demonstrated that NO derived from eNOS, but not from iNOS, contributes to increase the mural cell coverage of B16 melanoma vessels.

S1P through the activation of S1P1, a G-protein-coupled receptor, induces NO synthesis through eNOS activation in ECs (37). In our experimental conditions, we showed that 2 different S1P1-blocking antibodies and an S1P1 antagonist inhibited the promigratory effect exerted by sVEGFR-1 and -2 on mural cells. In addition, through a PKC-dependent pathway, sVEGFR-1 and -2 promoted the overexpression of S1P1 in ECs, albeit in a lesser extent than PMA or VEGF. All these data evidence that the S1P/S1P1 axis is implicated in the promigratory effect induced by sVEGFR-1 and -2. At the present time, the promoter region of S1P1 gene has not been extensively characterized in ECs, and mechanistic insights how expression of S1P1 gene is determined are to be elucidated more in detail (47). Nevertheless, endothelial-specific S1P1-knockout mice exhibit mural vessel coverage defect, demonstrating that S1P/S1P1 signaling contributes to vessel stabilization (38).

We demonstrated that sVEGFR-1 and -2 were not only circulating VEGF sequestering proteins, but that they could bind to ECs. As illustrated in Fig. 9, these data support that, in addition to trapping VEGF at a circulating level, sVEGFRs could form a signaling-inactive membrane-associated complex consisting of sVEGFR/VEGF/VEGFR-2 that prevents VEGF-driven angiogenesis. They could also bind ECs through interaction with a coreceptor that could subsequently gen-

erate a trans-signaling similar to what is observed for soluble IL-6 receptor (48). In addition, if they completely trapped free VEGF and abrogated VEGF-driven proliferation, migration, differentiation, and angiogenesis, they could not completely inhibit VEGFR-2 and eNOS phosphorylation in ECs. This paradox could be explained by the presence of an intracrine VEGF pathway. Indeed, using mice where VEGF was specifically deleted in ECs, Lee *et al.* (49) demonstrated that VEGF acts as an intracrine factor that is crucial for vascular homeostasis. Their findings uncovered an important role for intracrine VEGF signaling in survival mechanisms following hypoxia-mediated stress for which paracrine sources of VEGF cannot compensate. This intracrine VEGF/VEGFR-2 pathway, which remains and signals inside ECs, could be recruited when ECs are deprived of exogenous VEGF by sVEGFR-1 or -2. Moreover, we did not observe any mural cell outgrowth in the aortic ring assay when using an inhibitor that blocks both cytoplasmic membrane-associated VEGFR-2 and intracrine VEGFR-2 signaling. These results support that a residual kinase activity of endothelial VEGFR-2 is necessary to observe the mural cell recruitment induced by sVEGFR-1 and -2. They reconcile our data with the study of Igarashi (47), which described that S1P1 could be up-regulated by VEGF. Finally, they underline how the function of a cell is finely driven by the accurate regulation of its signaling level.

Collectively, our data indicate that when immature endo-

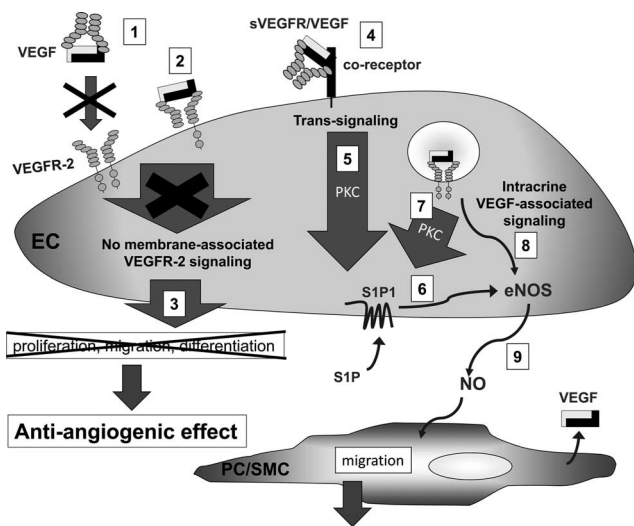


Figure 10. Model of VEGF family contribution to EC-PC/SMC dialogue. In addition to trapping VEGF at a circulating level (1), sVEGFR-1 and -2 could form a signaling-inactive membrane-associated complex consisting of sVEGFR/VEGF/VEGFR-2 (2), both ending to prevent VEGF-driven angiogenesis (3). They could also bind ECs through interaction with a coreceptor (4) that engaged a PKC-dependent trans-signaling (5) up-regulating S1P1 expression and thus favoring eNOS activation through the S1P/S1P1 pathway (6). Intracrine VEGF-associated signaling could up-regulate S1P1 expression through a PKC-dependent pathway (7), thus favoring eNOS activation through the S1P/S1P1 pathway (6) and/or could directly promote eNOS phosphorylation (8). The subsequent NO release induced the migration of neighbor PC/SMCs (9), thus promoting mural cells recruitment.

thelium is bathed with sVEGFR-1 or -2 and thus deprived of circulating VEGF, the proliferative phase of angiogenesis is stopped, and the mural cell recruitment is engaged to end to vessel maturation. In these conditions, the recruitment of mural cells results from interplay between VEGF/VEGFR-2 and S1P/S1P1 pathways that lead to eNOS activation. Indeed, our data support the following mechanisms of molecular interactions summarized in Fig. 10: 1) in addition to trapping VEGF at a circulating level, sVEGFR-1 and -2 could form a signaling-inactive membrane-associated complex consisting of sVEGFR/VEGF/VEGFR-2 both ending to prevent VEGF-driven angiogenesis, 2) a PKC-dependent trans-signaling resulting from the binding of sVEGFR/VEGF to a membrane coreceptor could up-regulate S1P1 expression and thus favoring eNOS activation through the S1P/S1P1 pathway, 3) intracrine VEGF-associated signaling could up-regulate S1P1 expression through a PKC-dependent pathway, and 4) intracrine VEGF-associated signaling could also directly promote the phosphorylation of eNOS. Our data complete the study of Greenberg *et al.* (50), who described that VEGF was a direct inhibitor of PC function and vessel maturation. Indeed, they demonstrated that, in mural cells, the VEGF-mediated activation of VEGFR-2 inhibited PDGFR- β signaling through the formation of a receptor complex consisting of VEGFR-2 and PDGFR- β . In turn this reduced the mural cell migration. In line with our data, overexpression of sVEGFR-1 and -2 would reduce the formation of such complex and sustain PDGF-BB-

dependent mural cell migration. Our results are also in line with the observations of Mazzone *et al.* (6), who have shown that an increase of vessel stabilization is associated with the enhancement of sVEGFR-1 expression by quiescent ECs of newly formed capillaries. In this location the sVEGFR-1 would, as demonstrated here, inhibit the EC proliferation and migration and enhance mural cell coverage and vessel maturation.

In summary, we demonstrated here that sVEGFR-1 and -2 take part in vessel maturation *via* the induction of mural cell recruitment through a paracrine effect involving ECs. Our findings support the idea that endogenously produced sVEGFR-1 and exogenously administrated sVEGFR-1/Fc or sVEGFR-2/Fc regulate the balance between pro- and antiangiogenic factors and that they are involved in the formation of a stable vasculature by inducing mural cell migration. In the context of the currently used anti-VEGF therapies, our results contribute to clarify clinical observations where agents targeting the VEGF pathway induce a transient “normalization” of tumor vessels by increasing their mural cell coverage. Normalization of tumor vasculature is an emerging strategy to improve radiation and cytotoxic therapies (36). Contribution of soluble VEGFRs may ultimately prove beneficial for normalizing tumoral vasculature and improving the response to radiation and chemotherapy. [FJ]

The authors thank B. Brouwers, I. Dasoul, D. Gabriel-Delapierre, N. Lefin, M.-R. Pignon, E. Konradowski, F. Olivier, P. Gavittelli, and G. Rolland for their excellent technical assistance. Confocal microscopy was performed at CIL- and GIGA-Imaging and Flow Cytometry Facility. This work was supported by grants from the European 7th Research Framework Programme: HEALTH-2007-2.4.1-6 “MICROENVIMET,” Framework Programme 6-NOE LSHM-CT-2004-512040, EMBIC, the Fonds de la Recherche Scientifique Médicale, the Fonds National de la Recherche Scientifique (FNRS; Belgium), the Fondation contre le Cancer, the Fonds spéciaux Recherche (University of Liège), the Centre Anticancéreux près l’Université de Liège, the Fonds Léon Fredericq (University of Liège), the DGTRE from the Région Wallonne (NEOANGIO), the Fonds Social Européen, and the Interuniversity Attraction Poles Programme–Belgian Science Policy (Brussels, Belgium). S.L. and C.P. performed all cellular experiments; S. Berndt performed the aortic ring assays; S. Blacher did all quantification based on image analysis; E.G. contributed to the mouse Matrigel plug assay; O.P., E.M., and A.N. contributed to the work with scientific advice; J.-M.F. supervised the study, provided scientific suggestions, and contributed to manuscript preparation and review; C.M. participated to data analysis; and C.P. designed the study, analyzed the data, and wrote the manuscript.

REFERENCES

- Carmeliet, P. (2005) Angiogenesis in life, disease and medicine. *Nature* **438**, 932–936
- Jain, R. K. (2005) Normalization of tumor vasculature: an emerging concept in antiangiogenic therapy. *Science* **307**, 58–62
- Sullivan, R., and Graham, C. H. (2007) Hypoxia-driven selection of the metastatic phenotype. *Cancer Metastasis Rev.* **26**, 319–331
- Fukumura, D., and Jain, R. K. (2007) Tumor microvasculature and microenvironment: targets for anti-angiogenesis and normalization. *Microvasc. Res.* **74**, 72–84

5. Gerhardt, H., and Symb, H. (2008) Pericytes: gatekeepers in tumour cell metastasis? *J. Mol. Med.* **86**, 135–144
6. Mazzone, M., Dettori, D., Leite de Oliveira, R., Loges, S., Schmidt, T., Jonckx, B., Tian, Y. M., Lanahan, A. A., Pollard, P., Ruiz de Almodovar, C., De Smet, F., Vinckier, S., Aragonés, J., Debackere, K., Luttun, A., Wyns, S., Jordan, B., Pisacane, A., Gallez, B., Lampugnani, M. G., Dejana, E., Simons, M., Ratcliffe, P., Maxwell, P., and Carmeliet, P. (2009) Heterozygous deficiency of PHD2 restores tumor oxygenation and inhibits metastasis via endothelial normalization. *Cell* **136**, 839–851
7. Chabottaux, V., Ricaud, S., Host, L., Blacher, S., Paye, A., Thiry, M., Garofalakis, A., Pestourie, C., Gombert, K., Bruyère, F., Lewandowsky, D., Tavittian, B., Foidart, J.-M., Duconge, F., and Noël, A. (2009) A membrane-type 4 matrix metalloproteinase (MT4-MMP) induces lung metastasis by alteration of primary breast tumor vascular architecture. *J. Cell. Mol. Med.* **13**, 4002–4013
8. Tong, R. T., Boucher, Y., Kozin, S. V., Winkler, F., Hicklin, D. J., and Jain, R. K. (2004) Vascular normalization by vascular endothelial growth factor receptor 2 blockade induces a pressure gradient across the vasculature and improves drug penetration in tumors. *Cancer Res.* **64**, 3731–3736
9. Winkler, F., Kozin, S. V., Tong, R. T., Chae, S. S., Booth, M. F., Garkavtsev, I., Xu, L., Hicklin, D. J., Fukumura, D., di Tomaso, E., Munn, L. L., and Jain, R. K. (2004) Kinetics of vascular normalization by VEGFR2 blockade governs brain tumor response to radiation: role of oxygenation, angiopoietin-1, and matrix metalloproteinases. *Cancer Cell* **6**, 553–563
10. Bergers, G., and Hanahan, D. (2008) Modes of resistance to anti-angiogenic therapy. *Nat. Rev. Cancer* **8**, 592–603
11. Jain, R. K. (2003) Molecular regulation of vessel maturation. *Nat. Med.* **9**, 685–693
12. Armulik, A., Abramsson, A., and Betsholtz, C. (2005) Endothelial/pericyte interactions. *Circ. Res.* **97**, 512–523
13. Andrae, J., Gallini, R., and Betsholtz, C. (2008) Role of platelet-derived growth factors in physiology and medicine. *Genes Dev.* **22**, 1276–1312
14. Kashiwagi, S., Izumi, Y., Gohongi, T., Demou, Z. N., Xu, L., Huang, P. L., Buerk, D. G., Munn, L. L., Jain, R. K., and Fukumura, D. (2005) NO mediates mural cell recruitment and vessel morphogenesis in murine melanomas and tissue-engineered blood vessels. *J. Clin. Invest.* **115**, 1816–1827
15. Peters, S. L. M., and Alewijnse, A. E. (2007) Sphingosine-1-phosphate signaling in the cardiovascular system. *Curr. Opin. Pharmacol.* **7**, 186–192
16. Allende, M. L., and Proia, R. L. (2002) Sphingosine-phosphate receptors and the development of the vascular system. *Biochim. Biophys. Acta* **1582**, 222–227
17. Kono, M., Mi, Y., Liu, Y., Sasaki, T., Allende, M. L., Wu, Y. P., Yamashita, T., and Proia, R. L. (2004) The sphingosine-1-phosphate receptors S1P1, S1P2, and S1P3 function coordinately during embryonic angiogenesis. *J. Biol. Chem.* **279**, 29367–29373
18. Shibuya, M. (2006) Differential roles of vascular endothelial growth factor receptor-1 and receptor-2 in angiogenesis. *J. Biochem. Mol. Biol.* **39**, 469–478
19. Swendeman, S., Mendelson, K., Weskamp, G., Horiuchi, K., Deutsch, U., Scherle, P., Hooper, A., Rafii, S., and Blobel, C. P. (2008) VEGFA stimulates ADAM17-dependent shedding of VEGFR2 and crosstalk between VEGFR2 and ERK signaling. *Circ. Res.* **103**, 916–918
20. Ebos, J. M., Bocci, G., Man, S., Thorpe, P. E., Hicklin, D. J., Zhou, D., Jia, X., and Kerbel, R. S. (2004) A naturally occurring soluble form of vascular endothelial growth factor receptor 2 detected in mouse and human plasma. *Mol. Cancer Res.* **2**, 315–326
21. Kou, B., Li, Y., Zhang, L., Zhu, G., Wang, X., Li, Y., Xia, J., and Shi, Y. (2004) In vivo inhibition of tumor angiogenesis by a soluble VEGFR-2 fragment. *Exp. Mol. Pathol.* **76**, 129–137
22. Jacobi, J., Tam, B. Y., Wu, G., Hoffman, J., Cooke, J. P., and Kuo, C. J. (2004) Adenoviral gene transfer with soluble vascular endothelial growth factor receptors impairs angiogenesis and perfusion in a murine model of hindlimb ischemia. *Circulation* **110**, 2424–2429
23. Szentirmai, O., Baker, C. H., Bullain, S. S., Lin, N., Takahashi, M., Folkman, J., Mulligan, R. C., and Carter, B. S. (2008) Successful inhibition of intracranial human glioblastoma multi-forme xenograft growth via systemic adenoviral delivery of soluble endostatin and soluble vascular endothelial growth factor receptor-2: laboratory investigation. *J. Neurosurg.* **108**, 979–988
24. Tsatsaris, V., Goffin, F., and Foidart, J. M. (2004) Circulating angiogenic factors and preeclampsia. *N. Engl. J. Med.* **350**, 2003–2004; author reply 2003–2004
25. Munaut, C., Lorquet, S., Pequeux, C., Blacher, S., Berndt, S., Franckne, F., and Foidart, J. M. (2008) Hypoxia is responsible for soluble vascular endothelial growth factor receptor-1 (VEGFR-1) but not for soluble endoglin induction in villous trophoblast. *Hum. Reprod.* **23**, 1407–1415
26. Robak, E., Sysa-Jedrzejewska, A., and Robak, T. (2003) Vascular endothelial growth factor and its soluble receptors VEGFR-1 and VEGFR-2 in the serum of patients with systemic lupus erythematosus. *Mediators Inflamm.* **12**, 293–298
27. Wierzbowska, A., Robak, T., Wrzesien-Kus, A., Krawczynska, A., Lech-Maranda, E., and Urbanska-Rys, H. (2003) Circulating VEGF and its soluble receptors sVEGFR-1 and sVEGFR-2 in patients with acute leukemia. *Eur. Cytokine Netw.* **14**, 149–153
28. Kearney, J. B., Kappas, N. C., Ellerstrom, C., DiPaola, F. W., and Bautch, V. L. (2004) The VEGF receptor flt-1 (VEGFR-1) is a positive modulator of vascular sprout formation and branching morphogenesis. *Blood* **103**, 4527–4535
29. Kappas, N. C., Zeng, G., Chappell, J. C., Kearney, J. B., Hazarika, S., Kallianos, K. G., Patterson, C., Annex, B. H., and Bautch, V. L. (2008) The VEGF receptor Flt-1 spatially modulates Flk-1 signaling and blood vessel branching. *J. Cell Biol.* **181**, 847–858
30. Chappell, J. C., Taylor, S. M., Ferrara, N., and Bautch, V. L. (2009) Local guidance of emerging vessel sprouts requires soluble Flt-1. *Dev. Cell.* **17**, 377–386
31. Berndt, S., Perrier d'Hauterive, S., Blacher, S., Pequeux, C., Lorquet, S., Munaut, C., Applanat, M., Herve, M. A., Lamande, N., Corvol, P., van den Brule, F., Franckne, F., Poutanen, M., Huhtaniemi, I., Geenen, V., Noel, A., and Foidart, J. M. (2006) Angiogenic activity of human chorionic gonadotropin through LH receptor activation on endothelial and epithelial cells of the endometrium. *FASEB J.* **20**, 2630–2632
32. Masson, V. V., Devy, L., Grignet-Debrus, C., Bernt, S., Bajou, K., Blacher, S., Roland, G., Chang, Y., Fong, T., Carmeliet, P., Foidart, J. M., and Noel, A. (2002) Mouse aortic ring assay: a new approach of the molecular genetics of angiogenesis. *Biol. Proceed. Online* **4**, 24–31
33. Bruyere, F., Melen-Lamalle, L., Blacher, S., Roland, G., Thiry, M., Moons, L., Franckne, F., Carmeliet, P., Alitalo, K., Libert, C., Sleeman, J. P., Foidart, J. M., and Noel, A. (2008) Modeling lymphangiogenesis in a three-dimensional culture system. *Nat. Methods* **5**, 431–437
34. Passaniti, A., Taylor, R. M., Pili, R., Guo, Y., Long, P. V., Haney, J. A., Pauly, R. R., Grant, D. S., and Martin, G. R. (1992) A simple, quantitative method for assessing angiogenesis and antiangiogenic agents using reconstituted basement membrane, heparin, and fibroblast growth factor. *Lab. Invest.* **67**, 519–528
35. Yu, J., deMuinck, E. D., Zhuang, Z., Drinane, M., Kauser, K., Rubanyi, G. M., Qian, H. S., Murata, T., Escalante, B., and Sessa, W. C. (2005) Endothelial nitric oxide synthase is critical for ischemic remodeling, mural cell recruitment, and blood flow reserve. *Proc. Natl. Acad. Sci. U. S. A.* **102**, 10999–11004
36. Kashiwagi, S., Tsukada, K., Xu, L., Miyazaki, J., Kozin, S. V., Tyrrell, J. A., Sessa, W. C., Gerweck, L. E., Jain, R. K., and Fukumura, D. (2008) Perivascular nitric oxide gradients normalize tumor vasculature. *Nat. Med.* **14**, 255–257
37. Igarashi, J., Bernier, S. G., and Michel, T. (2001) Sphingosine 1-phosphate and activation of endothelial nitric-oxide synthase: differential regulation of Akt and MAP kinase pathways by EDG and bradykinin receptors in vascular endothelial cells. *J. Biol. Chem.* **276**, 12420–12426
38. Allende, M. L., Yamashita, T., and Proia, R. L. (2003) G-protein-coupled receptor S1P1 acts within endothelial cells to regulate vascular maturation. *Blood* **102**, 3665–3667
39. Igarashi, J., and Michel, T. (2008) S1P and eNOS regulation. *Biochim. Biophys. Acta* **1781**, 489–495
40. Kendall, R. L., and Thomas, K. A. (1993) Inhibition of vascular endothelial cell growth factor activity by an endogenously

- encoded soluble receptor. *Proc. Natl. Acad. Sci. U. S. A.* **90**, 10705–10709
41. Kamba, T., Tam, B. Y., Hashizume, H., Haskell, A., Sennino, B., Mancuso, M. R., Norberg, S. M., O'Brien, S. M., Davis, R. B., Gowen, L. C., Anderson, K. D., Thurston, G., Joho, S., Springer, M. L., Kuo, C. J., and McDonald, D. M. (2006) VEGF-dependent plasticity of fenestrated capillaries in the normal adult microvasculature. *Am. J. Physiol. Heart Circ. Physiol.* **290**, H560–H576
 42. Roeckl, W., Hecht, D., Sztajer, H., Waltenberger, J., Yayon, A., and Weich, H. A. (1998) Differential binding characteristics and cellular inhibition by soluble VEGF receptors 1 and 2. *Exp. Cell. Res.* **241**, 161–170
 43. Albuquerque, R. J., Hayashi, T., Cho, W. G., Kleinman, M. E., Dridi, S., Takeda, A., Baffi, J. Z., Yamada, K., Kaneko, H., Green, M. G., Chappell, J., Wilting, J., Weich, H. A., Yamagami, S., Amano, S., Mizuki, N., Alexander, J. S., Peterson, M. L., Brekken, R. A., Hirashima, M., Capoor, S., Usui, T., Ambati, B. K., and Ambati, J. (2009) Alternatively spliced vascular endothelial growth factor receptor-2 is an essential endogenous inhibitor of lymphatic vessel growth. *Nat. Med.* **15**, 1023–1030
 44. Ferrara, N., and Kerbel, R. S. (2005) Angiogenesis as a therapeutic target. *Nature* **438**, 967–974
 45. Goldman, C. K., Kendall, R. L., Cabrera, G., Soroceanu, L., Heike, Y., Gillespie, G. Y., Siegal, G. P., Mao, X., Bett, A. J., Huckle, W. R., Thomas, K. A., and Curiel, D. T. (1998) Paracrine expression of a native soluble vascular endothelial growth factor receptor inhibits tumor growth, metastasis, and mortality rate. *Proc. Natl. Acad. Sci. U. S. A.* **95**, 8795–8800
 46. Dings, R. P., Loren, M., Heun, H., McNiel, E., Griffioen, A. W., Mayo, K. H., and Griffin, R. J. (2007) Scheduling of radiation with angiogenesis inhibitors anginex and Avastin improves therapeutic outcome via vessel normalization. *Clin. Cancer Res.* **13**, 3395–3402
 47. Igarashi, J., Erwin, P. A., Dantas, A. P., Chen, H., and Michel, T. (2003) VEGF induces S1P1 receptors in endothelial cells: implications for cross-talk between sphingolipid and growth factor receptors. *Proc. Natl. Acad. Sci. U. S. A.* **100**, 10664–10669
 48. Rose-John, S., Scheller, J., Elson, G., and Jones, S. A. (2006) Interleukin-6 biology is coordinated by membrane-bound and soluble receptors: role in inflammation and cancer. *J. Leukoc. Biol.* **80**, 227–236
 49. Lee, S., Chen, T. T., Barber, C. L., Jordan, M. C., Murdock, J., Desai, S., Ferrara, N., Nagy, A., Roos, K. P., and Iruela-Arispe, M. L. (2007) Autocrine VEGF signaling is required for vascular homeostasis. *Cell* **130**, 691–703
 50. Greenberg, J. I., Shields, D. J., Barillas, S. G., Acevedo, L. M., Murphy, E., Huang, J., Scheppke, L., Stockmann, C., Johnson, R. S., Angle, N., and Cheresch, D. A. (2008) A role for VEGF as a negative regulator of pericyte function and vessel maturation. *Nature* **456**, 809–813

Received for publication October 30, 2009.
Accepted for publication May 6, 2010.